21st Century Lunar Exploration: Advanced Radiation Exposure Assessment

Brooke Anderson, Martha Clowdsley, John Wilson
NASA Langley Research Center

John Nealy
Old Dominion University

Nathan Luetke
Lockheed Martin

ABSTRACT

On January 14, 2004 President George W Bush outlined a new vision for NASA that has humans venturing back to the moon by 2020. With this ambitious goal, new tools and models have been developed to help define and predict the amount of space radiation astronauts will be exposed to during transit and habitation on the moon. A representative scenario is used that includes a trajectory from LEO to a Lunar Base, and simplified CAD models for the transit and habitat structures. For this study galactic cosmic rays, solar proton events, and trapped electron and proton environments are simulated using new dynamic environment models to generate energetic electron, and light and heavy ion fluences. Detailed calculations are presented to assess the human exposure for transit segments and surface stays.

INTRODUCTION

In President Bush's new vision for NASA, humans are to venture back to the moon by 2020. Thus, work has begun in developing new tools and models to predict the space radiation exposure that astronauts will experience during the transit segments and habitation on the moon. This paper will describe the results of these new developments using a sample mission to the moon as the scenario. A simulated trajectory to the moon has been produced, as well as general CAD representations of a crew transfer vehicle (CTV) and a long term lunar habitat (LTLH). In addition to the trajectory and geometry, this analysis includes the three space radiation environments' fluences (trapped protons and electrons, GCR, and solar proton events) for inputs into the transport calculations. Thus, the predicted dose at specified locations within the crew transfer vehicle and habitat will be evaluated.

MISSION TIMELINE AND TRAJECTORY

The tool used to develop the trajectory is AGI's Satellite Tool Kit. In designing the trajectory,[1] it was assumed a parking orbit around Low Earth Orbit (LEO) would be the starting point, and then target the general vicinity of the moon, see figure 1. This was done with a target sequence using the delta declination and delta right ascension, the difference between the declination and right ascension of the spacecraft and the planet, as constraints and the launch epoch and coast time as control variables.

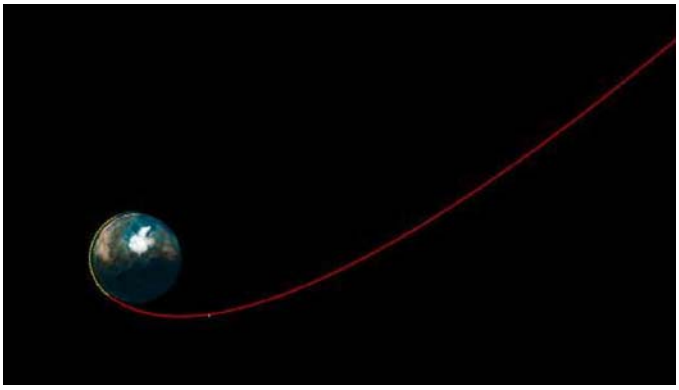

Figure 1. Depiction of outbound trajectory in vicinity of transit through trapped radiation belts.

Once in the general vicinity of the moon another target sequence was used to adjust the size of the Trans-Lunar Injection (TLI) impulsive maneuver to target the B-Plane of the moon. Then a final target sequence was used to perform the Lunar Orbit Insertion (LOI) by varying the LOI impulsive maneuver to get the desired location on the moon. The outbound trajectory can be seen in figure 2. The resulting trip time is 74 hours, with a total delta V of approximately 3 km/sec. Then a six month stay would ensue for research and or mining.

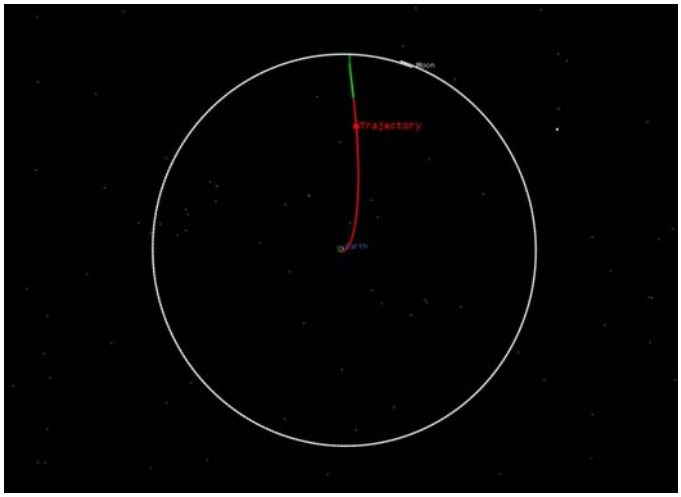

Figure 2. Depiction of complete trajectory.

SPACE RADIATION ENVIRONMENT DEFINITION

The first encounter with ionizing radiation along the outbound trajectory is that of the geomagnetically trapped protons and electrons in the near-earth vicinity. A computational procedure recently developed at NASA-Langley[2] was used to describe the time development of these high energy trapped particles. The differential energy spectra were calculated from trajectory positional data (time, altitude, latitude, and longitude in earth-centered frame) and the running summation evaluated to provide fluence as a function of time. The fluence spectra for trapped protons and electrons are shown in Figs. 3 and 4, respectively, for the initial stages of the outbound trajectory. The field of the trapped protons extends to ~3.5 R_E (earth radii), whereas the electron belt extends to ~9 R_E. Consequently, the total trapped proton fluence is reached in ~45 min. and that of electrons in 2 hr. 20 min. as shown in the plots. The fluence spectra as evolved for these time periods have been used in the subsequent transport calculations.

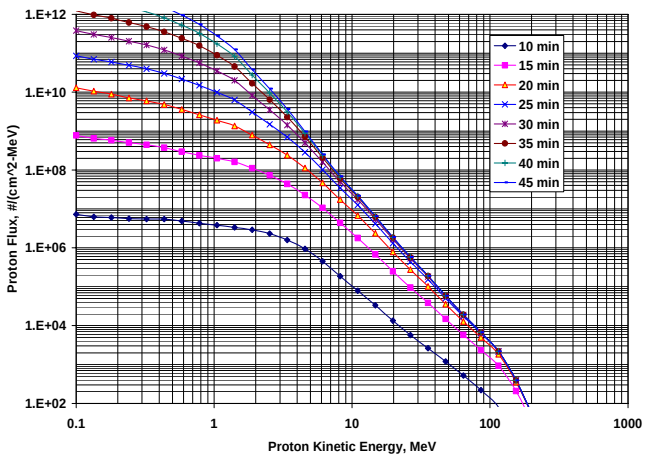

Figure 3. Successive proton fluence spectra for early segment of outbound trajectory.

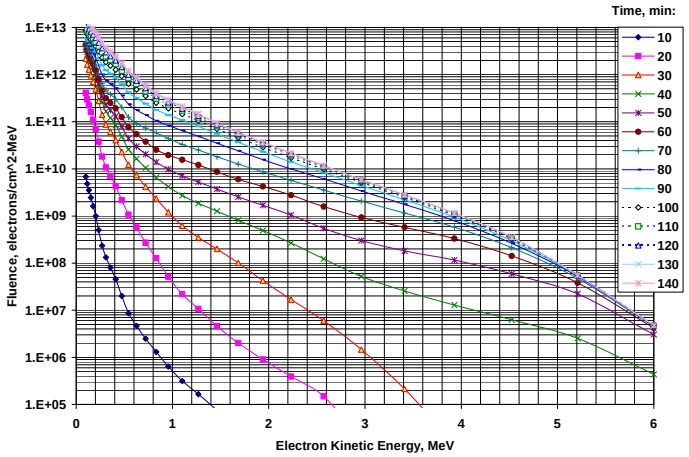

Figure 4. Successive electron fluence spectra for early segment of outbound trajectory.

Since the scenario has been chosen to correspond approximately to solar cycle maximum conditions, the possible effects of a large solar flare have been included in the analysis. The flare spectrum selected is that of August 1972, shown in Figure 5, and corresponds to the analysis of J. King[3]. It is noteworthy that this particular flare erupted within months of the flights of Apollo XVI and XVII – Apr. and Dec. 1972. Although such flares are rare, their hazard is great since an occurrence during a lunar mission could adversely affect mission operations.

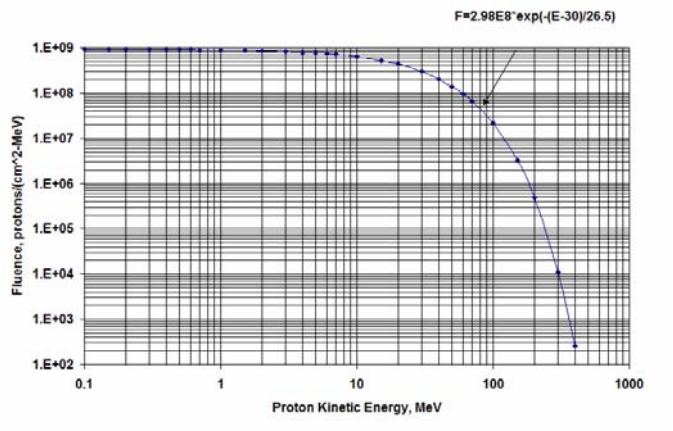

Figure 5. Differential fluence for August 1972 large solar flare.

Another relevant constituent of the interplanetary radiation field is that of the galactic cosmic rays (GCR), consisting of high energy atomic nuclei of the elements of composition roughly corresponding to their observed natural abundance. Hence, protons are most abundant, but the contributions to exposure from heavier elements (e. g. C, O, Si, and Fe) are notably significant in that their greater mass, charge and energy offset their lower flux in interactions with condensed matter. The GCR environment[4], and flux spectra for the first 28 elements are shown in Figure 6. The GCR are always present, with flux values about 3 times greater at solar minimum than at solar maximum. In the absence of large flare activity and relatively short times spent in the trapped belt regions, the GCR will dominate the exposure for a lunar mission. These particles, and especially their high energy secondaries, are capable of penetrating very thick shields, and some degree of exposure is practically unavoidable.

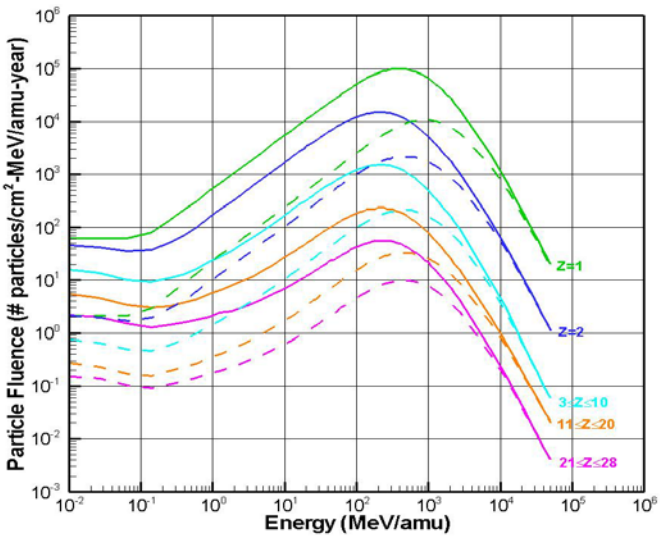

Figure 6. Annual galactic cosmic ray flux for solar minimum (solid) and maximum (dashed).

VEHICLE/HABITAT CAD MODEL DESCRIPTION

The crew transfer vehicle, (CTV) was modeled to simulate a larger version of the Apollo capsule, which is a possible concept for future missions to the moon. This model, seen in figure 7, was generated in the commercial CAD package I-DEAS, version 11. It has an overall diameter of 5.5 meters with inclined walls at an angle of 32 degrees with the horizontal. The outer shell is a 2.5 centimeter thick thermal protection layer encapsulating a much thicker 15 centimeter thick outer mold-line structure. The final internal layer is a 0.75 centimeter thick aluminum pressure vessel[5]. Inside of the CTV model are 5 crew chairs and several containers located in a circular pattern surrounding the seated crew location. Along with these features, the CTV also contains two helium tanks, two nitrogen tanks, three tanks of ethanol and five oxygen tanks. All five windows are two-layered fused silica with a mass of 3.7 kilograms per pane. There are two forward windows looking towards the CTV peak and two windows on either side of the main door which itself has one circular window. The CTV main door is similar to the Apollo main door; however it has a mass of 130% of that of Apollo's. This section of the CTV-Service module configuration has a total mass of 7,986 kilograms based on the Cycle four, block two configuration dry mass from table 5-1 of reference five. The second part of the configuration is the Service Module (SM), which consists simply of an outer 5 centimeter thick thermal protection layer wrapped around a 5 centimeter thick outer SM shell. Internally the SM has a six finned structure enclosing two helium tanks, two oxygen tanks and two methane tanks. Two 126 kilogram solar panels are also modeled. This section has a mass of 11,532 kilograms from table 5-2 in reference five based on ignoring the growth, non-cargo, avionics, environment and other masses along with the RCS thrusters due to incomplete information on these components. Two target points representing locations the crew would possibly spend most of their time were chosen for analysis and can be seen in figure 7. These points were ray traced and the resulting thickness amounts have been arranged in ascending order and normalized to form cumulative thickness distributions, which are shown in figure 8.

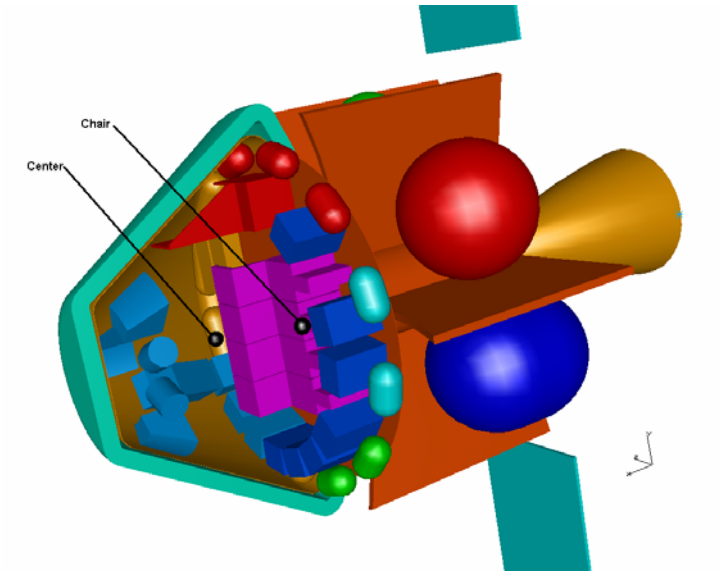

Figure 7. View of CAD model of a conceptual CTV, and selected target points.

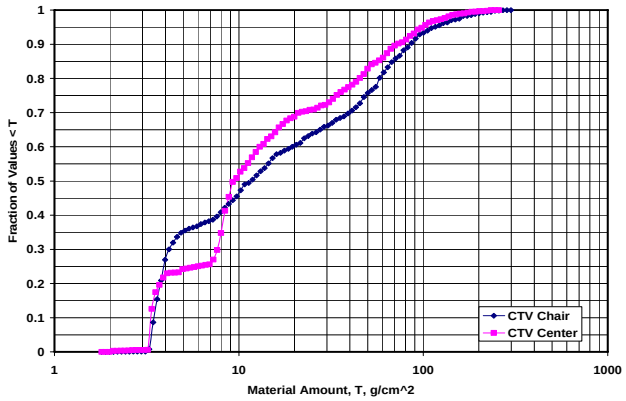

Figure 8. Cumulative distribution of inherent shield amounts for target points in CTV.

The Long Term Lunar Habitat (LTLH) model was also generated in I-DEAS 11 and can be seen in figure 9; it is modeled as a large cylindrical object approximately 23 meters high and was based upon the L1 Lunar Mission Architecture[6]. It consists of a 10 centimeter thick outer structure enclosing a three-floor layout. The top floor contains four crew quarters, a wash station and galley. Directly below this floor is the Habitat's laboratory which includes three tables and a storage container in this design. The two floors currently described are also enclosed in an additional 25 centimeter thick structure for added crew protection. The final floor that was modeled is the Extra Vehicular Activity (EVA) staging level which contains two rooms, utilizing 4.5 centimeter thick walls, with doors and a larger, yet thinner operations room which has a wall thickness of one centimeter. Below the bottom floor are modeled four propellant tanks and engines. The LTLH as presented here has a total mass of 16,518 kilograms. As can be seen in figure 9, three target points have been chosen for analysis, the thickness distribution of these target points can be seen in figure 10.

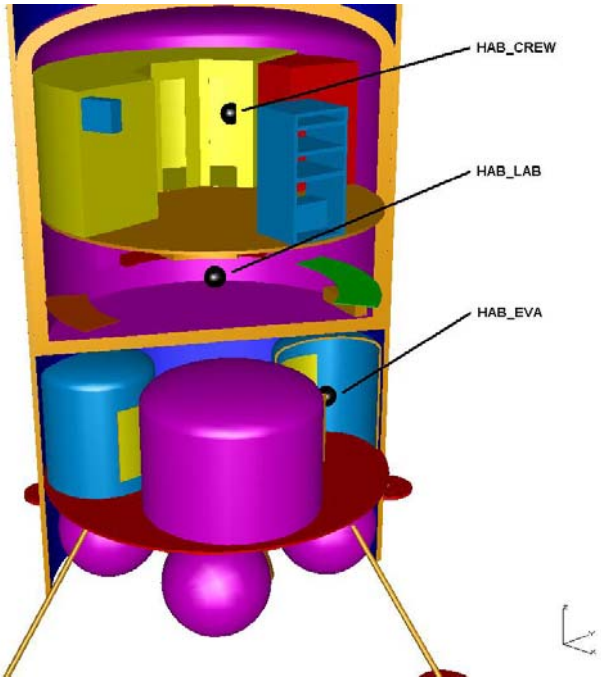

Figure 9. View of CAD-modeled conceptual lunar habitat showing interior target point locations.

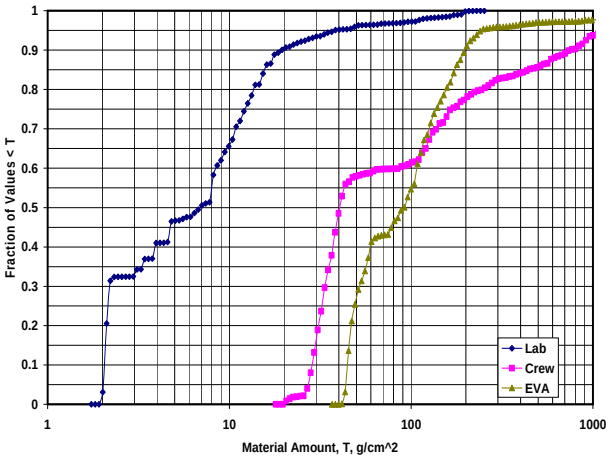

Figure 10. Cumulative distribution of inherent shield amounts for target points in LTLH.

HUMAN MODEL IMPLEMENTATION

The Computerized Anatomical Male (CAM) model was first developed by Kase[7] in 1970. Numerous errors were discovered in the combinatorial geometry, and Billings and Yucker[8] corrected the geometrical representation in 1973 using a QUAD geometry modeling technique[9] where geometrical regions and surfaces are used to represent the 50th percentile US Air Force male. The model is very detailed comprising some 1100 unique

geometric surfaces and approximately 2400 solid regions. The internal body geometry such as critical body organs, voids, bone, and bone marrow are explicitly modeled with the proper chemical composition and density. A supporting computer program called CAMERA was developed to perform analyses on the model, which include ray tracing to generate shielding distributions for any point in and on the CAM model. CAMERA also has the capability to generate cross-sectional views of the coordinate (dose) point of interest. The coordinate system's origin is at the top of the head with positive z downward, positive x toward the body front, and positive y toward the right.

For the present study, four skin target points and four Blood Forming Organs (BFO) points were chosen for analysis, along with a single eye (lens) point. The skin and eye thickness distributions are shown in figure 11 and the BFO thickness distributions are shown in figure 12. The particular target points were selected in order to reduce the computational requirements while representing a range of exposure values commensurate with an average body dose. Comprehensive calculations for a single environment spectrum using 42 distributed skin points and 32 BFO points have shown that this approach is accurate. The CAM coordinates of the chosen points are given in Table 1.

Table 1. CAM Target Points Used in Present Study

Location	Designation	x, cm	y, cm	z, cm
skin, right arm	*skn12*	-1.04	27.79	74.97
skin, right thigh (front)	*skn17*	9.24	8.88	111.89
skin, chest (front)	*skn22*	9.20	10.66	54.55
skin, derriere (left side)	*skn29*	-11.76	-12.52	94.69
eye, right ocular lens	*eye01*	8.62	3.162	10.92
BFO, sternum	*bfo06*	9.30	3.44	50.82
BFO, pelvis (center)	*bfo17*	0.48	-5.25	91.49
BFO, right femur	*bfo21*	3.82	8.59	119.39
BFO, pelvis (left side)	*bfo22*	0.59	-15.29	89.56

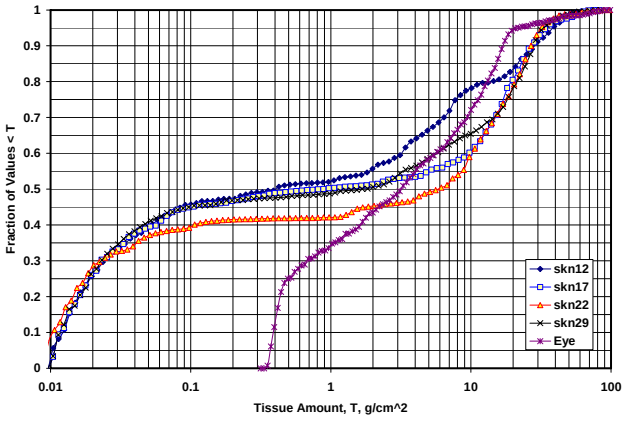

Figure 11. Cumulative thickness distributions for selected CAM skin and eye target points.

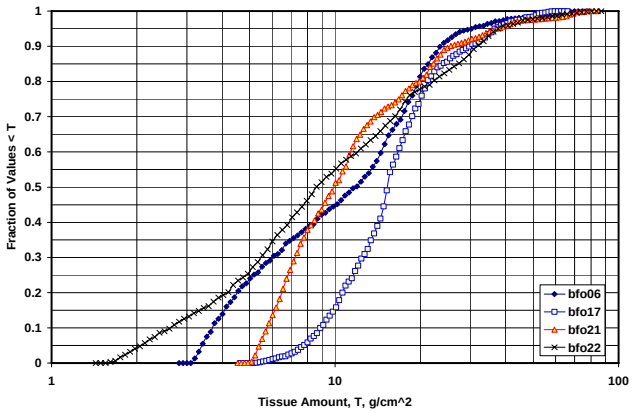

Figure 12. Cumulative thickness distributions for selected CAM BFO target points.

TRANSPORT CALCULATIONS FOR MATERIAL SHIELDING

Each of the radiation environment fluence energy spectra were used as boundary conditions for a range of shield material amounts followed by a range of body tissue amounts. Shield amounts have been scaled to g/cm^2 (thickness X density), with aluminum assumed for the primary shielding structure and with water used to simulate human tissue. For electrons, the transport computational code used was recently developed at NASA Langley and Old Dominion University[10] and for trapped protons, solar flare protons, and GCR ions, the deterministic code HZETRN[11] was utilized. In the case of trapped particles, the fluence envelope (uppermost curves in figures 3 and 4) were used as input for the transport codes. For the GCR, the HZETRN code was run for both solar maximum and minimum conditions, with the dose vs. depth curves corresponding to annual exposure at 1 A. U..

The exposure results for the array of Al + H_2O shield amounts for the trapped electrons are shown in figure 13. For very thin layers (~0.1 g/cm^2), the incurred dose may exceed 10 Sv (1 krad) due to the large flux of lower energy electrons. The plots indicate that for shield

amounts of ~1 to 2 g/cm^2, the electrons are essentially stopped, and for greater thicknesses the remaining brehmsstrahlung component attenuates more slowly. For the nominal crew-rated spacecraft, only these high energy photons contribute to the human exposure. For the trapped protons, the fluence spectra, shown in figure 14, are relatively "soft" (lacking in high energy particles) and subsequent exposures are also low for a nominally shielded structure. For the trajectory of this scenario, the trapped protons contribute negligibly to the overall human exposure.

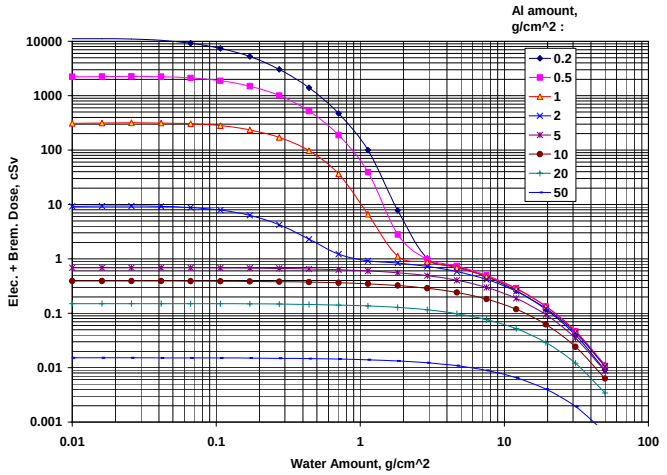

Figure 13. Dose vs. depth functions for mission trapped electron fluence.

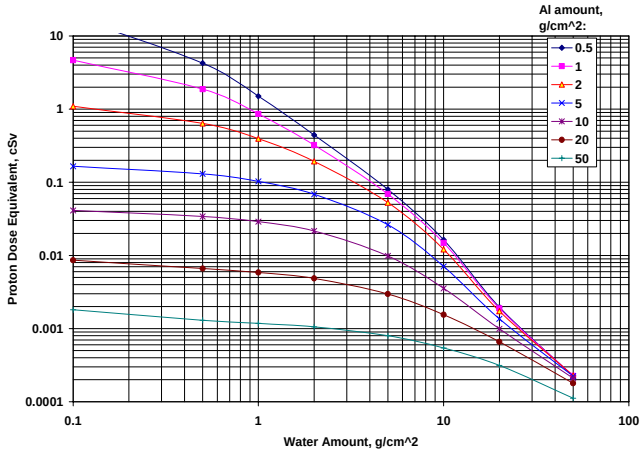

Figure 14. Dose vs. depth functions for mission trapped proton fluence.

The dose vs. depth array for the August 1972 solar flare is shown in figure 15. The results readily indicate that nominal shielding (~2 – ~5 g/cm^2) provides insufficient protection for humans. It has been established that nausea is initiated for dose values on the order of 1 Sv (100 rem), and the 50-percentile lethal dose is ~3 to ~4 Sv. A discussion of large dose effects on humans may be found in reference 11 (this conference). In the case of a lunar mission of only moderate duration, supplemental shielding that provides a "safe haven" for large flare protons should be a part of the mission infrastructure. Such arrangements may add substantial mass to a conceptual long-stay habitat, but can be accomplished so that potential flare dose risk can be reduced to acceptable levels.

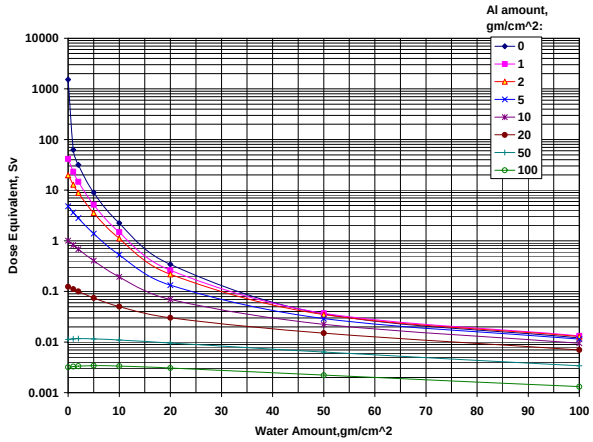

Figure 15. Dose vs. depth functions for large solar flare of Aug. 1972.

The transport calculations for GCR are presented in figures 16 and 17 for solar minimum and solar maximum, respectively. For these exposures, although 10 g/cm^2 or more shielding is highly desirable, the overall exposure as determined from mission duration is of the most importance. The effects produced by GCR are the long-term, stochastic induction of cancer, as opposed to the more immediate effects of large, sudden exposures from a solar flare. The GCR plots show that shield amounts greater than ~20 g/cm^2 provide relatively little additional attenuation.

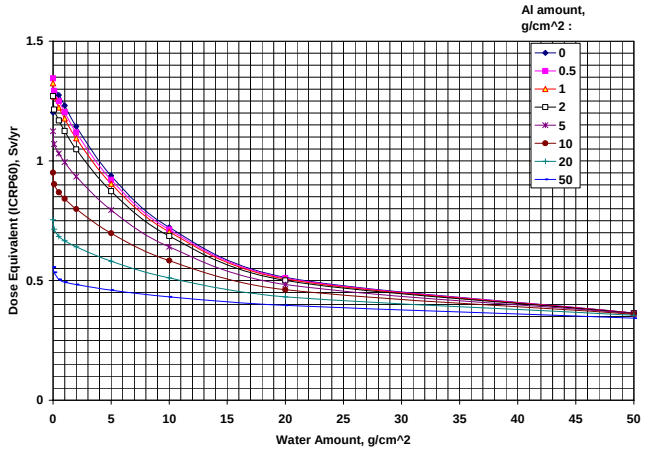

Figure 16. Dose vs. depth functions for annual GCR at solar minimum.

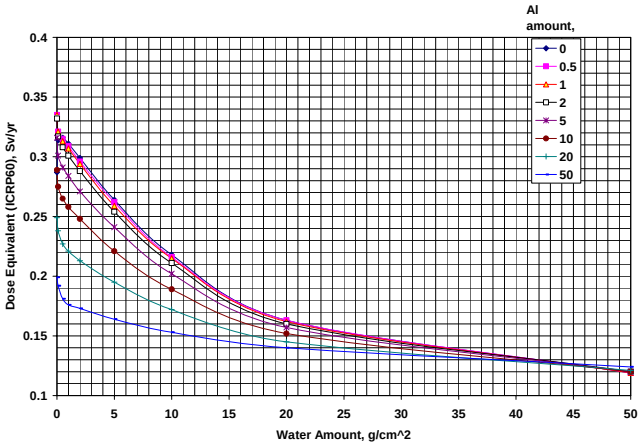

Figure 17. Dose vs. depth functions for annual GCR at solar maximum.

COMPUTATIONAL RESULTS FOR MISSION SCENARIO RADIATION EXPOSURES

Results of calculations of incurred dose equivalent at locations within the conceptual configurations for the specified CAM target points are given in Tables 2 and 3. Note that that the units are in Sieverts (Sv), and may be converted to the earlier rem units (cSv) with a multiplying factor of 100.

Table 2. CTV Calculated Dose Equivalent, Sv
Table 3. LTLH Calculated Dose Equivalent, Sv

Lab Area:

	gcrmin	gcrmax	Aug 72 flare
skn12	0.1821	0.0545	1.1535
skn17	0.1746	0.0531	1.0232
skn22	0.1725	0.0527	0.8859
skn29	0.1725	0.0527	0.9608
eye01	0.1795	0.0543	0.9317
bfo06	0.1588	0.0504	0.3375
bfo17	0.1438	0.0472	0.1234
bfo21	0.1548	0.0496	0.2611
bfo22	0.1616	0.0508	0.4555

Crew Quarters:

	gcrmin	gcrmax	Aug 72 flare
skn12	0.0694	0.0234	0.0058
skn17	0.0676	0.0230	0.0052
skn22	0.0678	0.0229	0.0050
skn29	0.0696	0.0235	0.0055
eye01	0.0674	0.0226	0.0055
bfo06	0.0682	0.0231	0.0044
bfo17	0.0695	0.0239	0.0038
bfo21	0.0698	0.0239	0.0045
bfo22	0.0679	0.0232	0.0044

EVA Airlock:

	gcrmin	gcrmax	Aug 72 flare
skn12	0.0750	0.0253	0.0030
skn17	0.0756	0.0256	0.0030
skn22	0.0759	0.0256	0.0030
skn29	0.0729	0.0248	0.0027
eye01	0.0749	0.0251	0.0031
bfo06	0.0760	0.0258	0.0030
bfo17	0.0761	0.0261	0.0027
bfo21	0.0765	0.0261	0.0029
bfo22	0.0743	0.0254	0.0027

For the CTV (Table 2), exposures from the trapped radiation belts (electrons + brehmsstrahlung, protons) are evaluated from the respective cumulative fluence envelopes during the belt transit. GCR contributions for the complete earth-moon trip have been evaluated for both solar min. and max. environments for the travel time of 3.08 days. It is readily seen from the results that, for the modeled CTV configuration, contributions from the trapped and GCR radiations are of little concern, whereas the large flare exposures indicate a potential mission-threatening (but still non-lethal) situation.

Seat Location:

	trapped e-	gcrmin	gcrmax	Aug 72 flare
skn12	0.0029	0.0048	0.0014	2.17
skn17	0.0033	0.0049	0.0015	2.62
skn22	0.0032	0.0049	0.0015	2.43
skn29	0.0014	0.0041	0.0013	0.64
eye01	0.0024	0.0049	0.0015	2.18
bfo06	0.0020	0.0044	0.0014	0.69
bfo17	0.0009	0.0039	0.0013	0.19
bfo21	0.0015	0.0042	0.0013	0.45
bfo22	0.0014	0.0041	0.0013	0.47

Center Location:

	trapped e-	gcrmin	gcrmax	Aug 72 flare
skn12	0.0024	0.0046	0.0014	1.45
skn17	0.0030	0.0049	0.0015	2.15
skn22	0.0027	0.0048	0.0015	1.81
skn29	0.0017	0.0044	0.0014	0.96
eye01	0.0023	0.0049	0.0015	1.69
bfo06	0.0017	0.0043	0.0014	0.54
bfo17	0.0009	0.0039	0.0013	0.17
bfo21	0.0013	0.0042	0.0013	0.35
bfo22	0.0015	0.0042	0.0014	0.50

Results for the two interior locations indicate that the central point offers somewhat better shielding than the seat location, but the differences are not remarkable. As expected, the results for GCR exhibit no great differences for any of the CAM body points, indicating that body self-shielding is not of great importance for these highly penetrating radiations.

Dose equivalent results for the LTLH (Table 3) include only the GCR and flare contributions. The previous descriptions of the three selected interior target points indicate well-shielded crew quarters and EVA-airlock areas, with the lab area having substantially less inherent shielding. The tabulated exposure calculations reflect results based on a six month stay time; 2π-steradian planetary shielding (below horizon) has been taken into account. It is seen that GCR dose rates are substantially reduced, particularly for the well-shielded locations; BFO dose rates, particularly in the lab area, would be of some concern (especially for longer stay times). Solar flare exposure values for the LTLH lab area are somewhat lower than for the CTV, but would remain of great concern. However, the crew quarters and EVA-airlock locations would provide entirely adequate "safe-haven" protection from such an event according to this particular modeled configuration.

CONCLUSION

Given a trajectory and models of the human and vehicles/habitats it is possible to predict the total space radiation dose with the newly developed and fully functional tools developed at Langley. For this scenario we choose an approximately 3 day trajectory to the moon and a 6 month stay on the moon. With the use of CAD models for the crew transfer vehicle and habitat, and the CAM model for the human representation, for the CTV we were able to predict that the trapped protons/electrons and the GCR will have little effect on the total dose but a solar flare such as the '72 event could pose a mission-threatening situation. As for the LTLH, several locations have substantially more shielding than the CTV but there are still more locations, such as the lab, that should be evaluated further if the astronauts tend to spend a large amount of operational time scheduled in these areas.

REFERENCES

1. AGI: "Beyond LEO: A Mission to the Moon", Retrieved November, 2005, Web site: http://www.agi.com/downloads/resources/download/tutorials/pdf/stk60/moonMission082505.pdf
2. Wilson, J. W.; Nealy, J. E.; De Angelis, G.; Badavi, F. F.; Hugger, C. P.; Cucinotta, F. A. and Kim, M. Y. (2003) "Dynamic/Anisotropic Low Earth Orbit Environment Models". Paper No. AIAA 2003-6221, SPACE 2003 Conf., Long Beach, CA.
3. King, J. H. (1974) "Solar Proton Fluences for 1977-1983 Space Missions". *J. Spacecraft*, 11, 401-408.
4. Badhwar, G. D. and O'Neill, P. M. (1996) "Galactic Cosmic Radiation Model and Its Applications". *Adv. Space Research,* 17, 7-17.
5. National Aeronautical and Space Administration (2005) "NASA's Exploration Systems Architecture Study." NASA TM 2005-214062.
6. Geffre, J. R. (2002) "Concept Design of a Lunar L1 Gateway Outpost," Paper No. IAA-13-2-04IAF. 34th COSPAR Scientific Assembly, the Second World Space Congress, Houston, TX.
7. Kase, Paul G. (1970) "Computerized Anatomical Model man," Report AFWL-TR-69-161, Air Force Weapons Laboratory, Kirkland Air Force Base, NM.
8. Billings, M.P. and Yucker, W.R. (1973) "Summary Final Report. The Computerized Anatomical Man (CAM) Model," Report MDC G4655, McDonnell Douglas Astronautics Company, Huntington Beach, CA.
9. Jordan, T.M. (1964) "QUAD, A Computer Subroutine for Ray Tracing in Quadric Surface Geometries," Douglas Report SM-46333.
10. Nealy, J. E.; Anderson, B. M.; Cucinotta, F. A.; Wilson, J. W.; Katz, R. and Chang, C. K. (2002) "Transport of Space Environment Electrons: A Simplified Rapid-Analysis Computational Procedure". NASA TP 2002-211448.
11. Wilson, J. W.; Tripathi, R. K.; Badavi, F. F. and Cucinotta, F. A. (2006) "Standardized Radiation Shield Design Method: 2005 HZETRN". Paper No. 06ICES-18, 36th International Conference on Environmental Systems, Norfolk, VA.